Review Article

Gerd Bramerdorfer*, Martin Kitzberger, Daniel Wöckinger, Branko Koprivica, and Stan Zurek

State-of-the-art and future trends in soft magnetic materials characterization with focus on electric machine design – Part 2

Stand der Technik und Trends im Bereich der Charakterisierung weichmagnetischer Materialien mit Fokus auf den Entwurf elektrischer Maschinen – Teil 2

https://doi.org/10.1515/teme-2019-0066
Received April 30, 2019; accepted June 23, 2019

Abstract: The first part of this two-part article is about a retrospective view of material characterization, starting with the work of J. Epstein around the year 1900 and respective basic explanations. Consequently, the work presented herein is about the current state-of-the-art, recent developments, and future trends in characterization of ferromagnetic materials. Modeling is in fact a type of characterization, in a phenomenological and mathematical sense, and therefore it is treated with due attention in this article. Quantifying the properties of soft magnetic materials retains significant scientific attention. Thanks to new optimization techniques and advances in numerical evaluation, modern electromagnetic devices feature high utilization. Classical models exhibit assumptions that do not allow modern machine or device characterization with high accuracy. In this manuscript, typically applied techniques and recent incremental improvements, as well as newly developed models are introduced and discussed. Moreover, the significant impact of manufacturing on the materials' characteristics and its quantification is illustrated. Within this article, a broad overview of the state-of-the-art as well as recent advances and future trends in soft magnetic material characterization is presented. Thus, it is a valuable reading for beginners and experts, from academia and industry alike.

Keywords: Iron losses, soft magnetic materials, ferromagnetic materials, initial magnetization curve, eddy current, hysteresis, degradation, manufacturing impact.

Zusammenfassung: Der erste Teil dieses zweiteiligen Artikels handelt von den anfänglichen Werken von J. Epstein um 1900 und einleitenden Erklärungen zu gängigen Messvorrichtungen. Darauf aufbauend werden hier neueste Entwicklungen und zukünftige Trends im Bereich der Materialcharakterisierung präsentiert. Die Quantifizierung der Eigenschaften weichmagnetischer Materialien erfuhr in letzter Zeit eine gesteigerte Bedeutung. Aufgrund neuer Optimierungstechniken und Fortschritten im Bereich numerischer Verfahren, werden heutzutage höchsteffiziente elektromagnetische Apparate entwickelt. Klassische Modellierungsverfahren wurden auf der Basis von grundlegenden Annahmen, wie sinusförmigen Flussdichteverläufen, entwickelt. Diese Annahmen sind heutzutage nicht mehr im vollen Umfang zutreffend, weshalb eine genaue Bewertung der Effizienz und Qualität elektrischer Maschinen oder Aktuatoren nicht mehr möglich ist. Dieser Artikel behandelt typische Modellierungsverfahren, aktuelle Verbesserungsansätze von etablierten Modellen und auch von Grund auf neu entwickelte Techniken. Überdies wird der signifikante Einfluss der Materialbearbeitung auf die elektromagnetischen Eigenschaften und folglich auf die Performanz von Aktuatoren und elektrischen Maschinen thematisiert. Jüngste Anstrengungen zu dessen Berücksichtigung im Entwurfsprozess werden aufgezeigt. Zusammenfassend gibt dieser Artikel einen profunden Überblick über den aktuellen Stand der Technik, sowie jüngste Verbesserungen und zukünftige Trends in der Charakterisierung weichmagnetischer Materialien. Er ist daher sowohl für Neueinsteiger, als auch für Experten, sowie für Personen aus der akademischen Forschung,

***Corresponding author: Gerd Bramerdorfer,** Johannes Kepler University Linz, Department of Electrical Drives and Power Electronics, Altenbergerstraße 69, 4040 Linz, Austria, e-mail: gerd.bramerdorfer@jku.at
Martin Kitzberger, Daniel Wöckinger, Johannes Kepler University Linz, Department of Electrical Drives and Power Electronics, Altenbergerstraße 69, 4040 Linz, Austria
Branko Koprivica, University of Kragujevac, Faculty of Technical Sciences in Cacak, Svetog Save 65, 32000 Cacak, Serbia, ORCID: https://orcid.org/0000-0001-5014-6866
Stan Zurek, Megger Instruments Ltd, Archcliffe Road, CT17 9EN Dover, UK

aber auch für Ingenieure aus der industriellen Praxis wertvoll.

Schlagwörter: Eisenverluste, weichmagnetische Materialien, Neukurve, Wirbelströme, Hysterese, Materialschädigung, Herstellungseinflüsse.

1 Introduction

Significant effort continues to be made for more accurate modeling of soft magnetic materials for electric machine design. Besides a generally increasing interest, a fundamental reason is the practical need for more efficient and more compact machine designs. Due to their short end winding, nowadays very often electric machines with tooth wound coils are applied. A side effect is the increased number of harmonics with considerable magnitude in the air gap field. Initial loss models for ferromagnetic materials were developed assuming sinusoidal flux densities. As this is no longer valid, new approaches have to be focused upon. In addition, computational power significantly increased and beneficial optimization techniques for nonlinear problems were developed, e. g., evolutionary algorithms. Therefore, electromagnetic devices are optimized using sophisticated algorithms and numerical techniques for evaluation. As usually cost or specific performance ratios play a key role, highly-utilized components are derived and ferromagnetic materials are thus driven in the very nonlinear region. Hence, a large part of the components features saturation regarding electromagnetic quantities. Furthermore, impact of manufacturing processes becomes more significant. This article is organized as follows: Section 2 is about modeling techniques for quantifying the relationship of magnetic field intensity and magnetic flux density, as well as the losses that arise in ferromagnetic components due to a change of the magnetization state. While in some approaches the evaluation of both effects is combined, in other models these two aspects are separated. Starting from typically applied and well-established models, recent modifications and improvements for more accurate modeling are presented. Section 3 gives the advances for considering the manufacturing effect in the design of electric machines or electromagnetic devices. Two major steps in manufacturing can be observed that take effect on the characteristics of ferromagnetic materials. One deals with techniques for obtaining the desired shape of the device cross section out of sheets of laminated steel. The other one is about effects with reference to the stacking of multiple sheets and the pressing of a lamination stack into or on auxiliary components. For instance, the stator of electric machines is often pressed in a housing made of aluminum, while the rotor is mounted on a shaft. Manufacturing effects are thus multi-faceted as well as the considerable amount of research that is actually carried out in this field. Finally, Section 4 presents a summary and conclusions of all past and ongoing activities.

2 Modeling of the magnetization characteristics

In the last one hundred years, scientists and engineers developed many different methods for modeling the magnetic hysteresis loop of soft magnetic materials. In general, the magnetic hysteresis exhibits strongly nonlinear characteristics and its shape usually depends on the magnetization history, the actual magnetization state due to the magnitude of the external fields, but also on the respective gradients of the magnetic field quantities. Unknown environmental aspects such as the mechanical stress inside the material or the local temperature distribution further affect the shape of magnetic hysteresis. For this reason, models that describe the total hysteresis in all aforementioned cases are very complex, hard to apply in simulation software and require extensive measurement data for complete identification. In many numerical simulation tools, only highly simplified models are implemented. Often, the hysteretic behavior of the material and hence magnetization history as well as iron losses are neglected during electromagnetic field calculation and only the nonlinear relationship between magnetic flux density B and magnetic field strength H is considered in terms of the initial magnetization curve. Section 2.1 introduces a short overview about commonly used models for B-H curves to be applied, e. g., for FEM (Finite Element Method), MoM (Methods of Moments), and engineering software, such as SPICE (Simulation Program with Integrated Circuit Emphasis). In order to obtain precise simulation results despite considering simplified magnetization curves, iron losses are taken into account at the post processing stage. Numerous approaches were developed and the authors summarize the most prominent examples in Section 2.2. Consequently, Section 2.3 lists common hysteresis models that allow jointly characterizing the actual magnetization state due to the magnetization history as well as the iron losses. Section 2.4 combines the magnetization characteristics as well as the instantaneous iron power losses in one novel

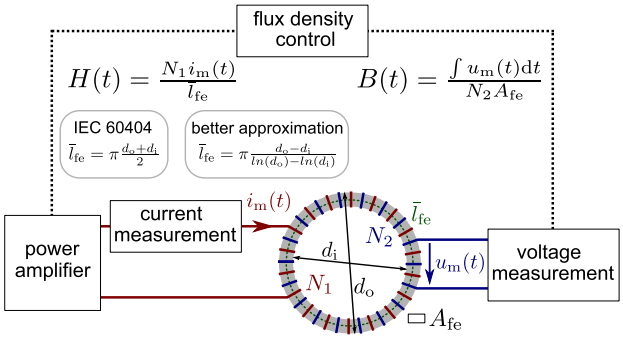

Figure 1: Schematic of an experimental setup consisting of a field coil with N_1 windings and an exploring coil with N_2 windings for a ring shaped specimen with an inner diameter of d_i, an outer diameter of d_o, a mean magnetic path length $\bar{l}_{fe}$, and a cross-sectional area of A_{fe}.

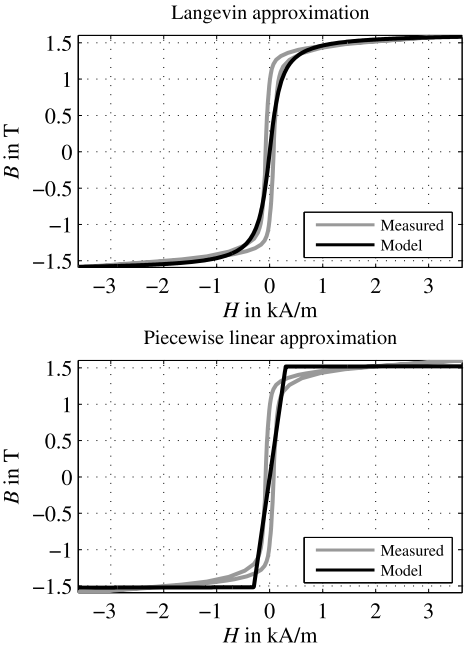

Figure 2: Measured hysteresis curve of a M250-35A electrical steel sheet with the experimental setup defined in [1] and its approximations using the Langevin function with the modeling parameters $B_s = 1.61\,\mathrm{T}$ and $a = 1.61\,\mathrm{A\,m^{-1}}$ (top figure). The piecewise linear approach with $B_s = 1.52\,\mathrm{T}$ and $\mu_a = 4000$ is illustrated in the bottom figure.

and powerful quasi time-invariant model. Finally, Section 2.5 gives a brief overview of the vector magnetic modeling of hysteresis and the iron losses for rotational magnetization.

2.1 Modeling of the B-H magnetization curve

Any modeling of B-H magnetization characteristics starts with acquiring data of the soft magnetic material under test. Obviously, the quality and accuracy of the derived model depends on the exactness of the provided B-H data. For this reason, many different measurement setups are established, e. g., the Epstein frame [23, 30], setups using ring-shaped specimens [1, 11, 32] or single sheet testers [64, 31]. The most relevant international standard for characterizing soft magnetic materials is IEC 60404. The values of B and H for all 1D measurement setups are derived based on auxiliary quantities. For instance, the current of the primary winding and the induced voltage of the secondary winding are used when considering the setup for ring-shaped specimens. Some assumptions are made, e. g., negligibly small stray flux, and no bias (DC) flux. Figure 1 illustrates a basic diagram of the measurement setup introduced in [11] for a ring-shaped specimen as well as the basic equations to determine the magnetic field quantities B and H from the measured primary current $i_m(t)$ and the detected secondary voltage $u_m(t)$. According to the international standard IEC60404 the magnetic path length $\bar{l}_{fe}$ is defined by using the average diameter of the ring-shaped specimen. For example, L. Chang describes in [14] another estimation of the mean magnetic path length to reach a better approximation of the resulting magnetic conditions inside the sample. Further details concerning the measuring setup can be found in [1, 11]. Regardless which setup is applied, one should always have the underlying assumptions in mind and evaluate if for the investigated test case, e. g., the saturation level and frequency considered, those assumptions are reasonable. A typical hysteresis curve for an M250-35A electrical steel sheet is illustrated in Fig. 2. Thereby, a sinusoidal waveform of B or H is investigated. The measured result is presented in grey color. Considering this initial situation, two different modeling approaches can be employed. On the one hand, many researchers use smoothing techniques to approximate the measured data. The applied functions are characterized by a very small number of parameters for representing the entire magnetic characteristics. On the other hand, piecewise defined functions are additionally applied that typically need a significant higher number of parameters. For the latter case, each part of the magnetization curve is defined by boundaries and individual curve parameters that are only valid in that particular curve section. The total number of modeling parameters is thus higher for a piecewise B-H curve definition compared to the smoothing techniques. A frequently applied modeling approach requiring only few parameters is based on the Langevin

function [45], which is defined as

$$B(H) = B_\mathrm{s}\left(\coth\left(\frac{H}{a}\right) - \frac{a}{H}\right). \tag{1}$$

B_s can be interpreted as the saturation magnetization of the specimen and a represents a material dependent parameter that is identified using measurement data. Furthermore, Wilson uses the arc-tangent function in [62] or Brauer in [13] utilizes an exponential function in order to model the measured B-H data. The variety of modeling approaches is widespread. Interested readers can find further formulations, e. g., rational or isoparametric approaches, in [18, 19, 47].

Depending on the considered material and thus on the shape of the B-H curve, an appropriate model can be selected in advance. Generally, all aforementioned models differ regarding the curve shape, the applicability considering numeric algorithms, but also on the number of model parameters to be determined. In contrast, in the simplest piecewise approximation a subdivision of the nonlinear magnetization curve into a linear region with high permeability μ_a and two areas of saturation is considered, such as

$$B(H) = \begin{cases} \mu_0 H & \mu_0\mu_\mathrm{a} H \geq B_\mathrm{s} \\ \mu_0\mu_\mathrm{a} H & -B_\mathrm{s} < \mu_0\mu_\mathrm{a} H < B_\mathrm{s} \\ \mu_0 H & \mu_0\mu_\mathrm{a} H \leq -B_\mathrm{s} \end{cases}. \tag{2}$$

In Fig. 2, the Langevin function and the simple piecewise model, respectively, are applied to fit the B-H curve of a specimen of M250-35A electrical steel. Although both models (1) and (2) use two material-specific parameters to describe the curve shape, the Langevin function (1) achieves a significantly higher accuracy. However, in contrast to that smooth approach, the precision of the piecewise linear B-H model can be significantly improved in two different ways. On the one hand, the number of regions, into which the curve is partitioned, can be increased. On the other hand, the complexity and thus the flexibility of the shape function can be increased. For example, Huelsmann describes in [29] an extended Brauer model that subdivides the magnetization curve into a quadratic so-called Rayleigh region, an exponentially approximated buckle, and finally a linear saturation area. A more general approach that uses a user-defined number of piecewise functions with higher-order terms can be found in [24]. In addition to preselection of the most appropriate model, another challenge is the estimation of the unknown modeling parameters. Usually, authors solve the problem of parameter identification by using optimization algorithms based on the least squares (LSQ)-method [37]. The modeling parameters for the approximated magnetization curves of M250-35A electrical steel in Fig. 2 are identified by such an algorithm as well.

2.2 Modeling of the losses due to changes in the magnetization state

To obtain the power loss through an entire cycle of a periodic change of the magnetization state, the size of the area spanned by the associated B-H loop needs to be evaluated. For 1D magnetization, the specific energy loss w_fe per volume and cycle can be defined as [44]

$$w_\mathrm{fe} = \oint_c H \,\mathrm{d}B. \tag{3}$$

The integral is assessed along the contour c of the material-specific B-H loop. In practice, the time-wise average of the power loss is of greater interest, which is defined as the specific energy loss averaged over time. It can be calculated as

$$p_\mathrm{fe} = f \oint_c H \,\mathrm{d}B. \tag{4}$$

Thus, p_fe gives the specific average power that is dissipated. In order to determine the instantaneous specific energy loss at any instant of time, (3) must be extended to

$$w_\mathrm{fe} = \int_{t_0}^{t_1} H(t)\frac{\mathrm{d}B(t)}{\mathrm{d}t}\,\mathrm{d}t, \tag{5}$$

where $[t_0, t_1]$ corresponds to the observed time interval. Consequently, the instantaneous specific power loss due to existence of lossy material is given as

$$p_\mathrm{fe}(t) = H(t)\frac{\mathrm{d}B(t)}{\mathrm{d}t}. \tag{6}$$

Throughout the next sections, the goal is to present widely applied iron loss models that take into account electromagnetic field quantities of the considered volume(s), the frequency of the applied change of magnetization and some further more or less material-specific parameters.

2.2.1 Iron loss models for alternating and purely sinusoidal flux densities

In many practical applications, a purely sinusoidal flux density in the material is considered. For this particular case, the well-known and empirically found Steinmetz equation [57]

$$p_\mathrm{fe} = C_\mathrm{s} f^\alpha \hat{B}^\beta \tag{7}$$

is typically used to determine the specific iron losses. Thereby, $\hat{B}$ denotes the magnitude of the sinusoidal mag-

netic flux density and f its frequency. The Steinmetz coefficients α, β and C_s are used to fit the model to the measured data. Generally, the values of the three Steinmetz coefficients themselves are frequency-dependent as well. This is why the loss estimation based on (7) provides decent accuracy only within a small frequency range, i. e. in the range of the frequency used for identification. Another quite different modeling approach is the loss separation principle, which subdivides the total specific iron loss in static hysteresis losses and dynamic eddy current losses [35]. The former represents the energy consumption that is needed for the expansion and contraction of the magnetic domains during a magnetization cycle at very low frequencies. Hence, it is assumed that the static losses scale linearly with the frequency of the remagnetization. The eddy current losses increase by the time derivative of the magnetic flux density squared. Thus, they grow with frequency squared for a sinusoidal temporal change of the respective field quantities. Consequently, the total specific iron losses can be calculated using

$$p_{\mathrm{fe}} = C_{\mathrm{hyst}} f \hat{B}^2 + C_{\mathrm{ec}} f^2 \hat{B}^2, \tag{8}$$

where C_{hyst} and C_{ec} are material specific weights that are determined to fit to the measured data, as for the Steinmetz coefficients in (7). Bertotti extends the separation approach by adding the excess losses [9], which follows

$$p_{\mathrm{fe}} = C_{\mathrm{hyst}} f \hat{B}^2 + C_{\mathrm{ec}} f^2 \hat{B}^2 + C_{\mathrm{exc}} f^{1.5} \hat{B}^{1.5}. \tag{9}$$

This third contribution to the total losses can be explained by the domain wall motion under alternating magnetization. Especially at very high frequencies, this term is getting important and should not be neglected any longer. In [65] this commonly used loss separation procedure is critically analyzed with focus on grain-oriented and non-oriented electrical steels that are utilized for many electromagnetic applications. Furthermore, the authors discuss the difficulties with skin effect definition in grain-oriented materials, but also show that the loss separation approach can offer very good accuracy for both sinusoidal and non-sinusoidal excitation. If no specific measurement data is available to determine the loss coefficients, engineers that develop electromagnetic devices need to rely on generic information provided in data sheets of the electric steel manufacturers. Often only the specific losses at a given operating point are specified. In these cases, the calculation of the specific loss p_{fe} for any other magnetic flux density magnitude $\hat{B}$ and frequency f can be done by scaling properties based on the loss separation approach (8) and (9)

$$p_{\mathrm{fe}} = p_{\mathrm{h}} \frac{f}{f_{\mathrm{n}}} \left(\frac{\hat{B}}{\hat{B}_{\mathrm{n}}} \right)^2 + p_{\mathrm{ec}} \left(\frac{f}{f_{\mathrm{n}}} \frac{\hat{B}}{\hat{B}_{\mathrm{n}}} \right)^2 \tag{10}$$

or

$$p_{\mathrm{fe}} = p_{\mathrm{h}} \frac{f}{f_{\mathrm{n}}} \left(\frac{\hat{B}}{\hat{B}_{\mathrm{n}}} \right)^2 + p_{\mathrm{ec}} \left(\frac{f}{f_{\mathrm{n}}} \frac{\hat{B}}{\hat{B}_{\mathrm{n}}} \right)^2 + p_{\mathrm{exc}} \left(\frac{f}{f_{\mathrm{n}}} \frac{\hat{B}}{\hat{B}_{\mathrm{n}}} \right)^{1.5}. \tag{11}$$

Thereby, the three coefficients p_{h}, p_{ec} and p_{exc} give the specific static hysteresis, eddy current and excess losses at a defined operating point $\hat{B}_{\mathrm{n}}$ and f_{n}. Standardized values for reference are $\hat{B}_{\mathrm{n}} = 1.5\,\mathrm{T}$ and $f_{\mathrm{n}} = 50\,\mathrm{Hz}$. In addition to the already discussed 1D alternating magnetization, at least some parts of electromagnetic devices are usually magnetized by a rotational field (of varying degree of ellipticity) such as the stator tooth of electrical machines or the T-joint parts in transformers. The physical mechanisms of loss formation are different for this type of magnetization. Thus, the aforementioned models hold only at very low frequencies as well as low amplitudes of B. Jacobs et al. [33] combined the model of loss separation due to (8) for alternating magnetization with an extra part for the rotational losses to

$$p_{\mathrm{fe}} = k_1 f \hat{B}^2 + f^2 \hat{B}^2 (k_2 + k_3 \hat{B}^{k_4}). \tag{12}$$

In (12) the parameter k_2 corresponds to the eddy current coefficient C_{ec} in (8), whereas k_1 includes, besides the hysteresis parameter C_{hyst}, an additional rotational hysteresis factor r and the minimum and maximum value of the magnetic flux density $B(t)$. The coefficients k_3 and k_4 improve the accuracy of the loss model for considerably high flux density levels. As mentioned before, all introduced models in this section are only valid for a purely sinusoidal temporal change of the magnetic flux density in the material. Furthermore, if the skin effect in the steel sheets cannot be neglected, models based on the separation approach (8) do not fit very well and high errors between model prediction and measurement of more than 200 % can occur [49].

2.2.2 Iron loss models for alternating non-sinusoidal *B* based on Steinmetz equation

Due to saturation effects in the materials, as well as due to non-sinusoidal excitation and the control of electromagnetic devices with PWM-based signals, the B waveform typically comprises multiple temporal harmonics with considerable magnitude. For this reason, the iron loss models of Section 2.2.1 often become significantly inaccurate. Severns considers higher harmonics in [51] by using the Fourier expansion of the magnetic flux density and apply (7) on each Fourier series component. Finally, the resulting iron losses of the particular harmonics are summed up to get the total iron loss of the waveform under consideration. According to this simple approach, the total iron losses for all imaginable magnetic flux density B wave-

forms can be estimated by

$$p_{\mathrm{fe}} = \sum_{n=0}^{\infty} C_{\mathrm{s}}(f_n) f_n^{\alpha} \hat{B}_n^{\beta} \tag{13}$$

or for a frequency-independent C_{s} by

$$p_{\mathrm{fe}} = C_{\mathrm{s}} \sum_{n=0}^{\infty} f_n^{\alpha} \hat{B}_n^{\beta} \tag{14}$$

However, the mathematical principle of superposition is only applicable for linear systems. Particular ferro- and ferrimagnetic materials exhibit strong nonlinear characteristics. Thus, the method of Fourier expansion does not hold in practice. In order to overcome this problem, further approaches based on the Steinmetz equation have been developed. According to (6) the instantaneous specific iron losses are directly proportional to the rated change of induction $\frac{\mathrm{d}B(t)}{\mathrm{d}t}$ that, in general, does not correspond to the fundamental frequency f. For this reason, in the Modified Steinmetz Equation (MSE) the frequency term in (7) is replaced by an equivalent frequency [49]

$$f_{\mathrm{eq}} = \frac{1}{2\pi\hat{B}^2} \int_0^T \left(\frac{\mathrm{d}B(t)}{\mathrm{d}t}\right)^2 \mathrm{d}t \tag{15}$$

where T is the periodic time of the fundamental wave. It constitutes a frequency that is equivalent to the rated change of the induction squared $\left(\frac{\mathrm{d}B(t)}{\mathrm{d}t}\right)^2$ averaged over the fundamental period. Consequently, the total iron losses appearing for a given waveform can be calculated using

$$p_{\mathrm{fe}} = C_{\mathrm{s}} f f_{\mathrm{eq}}^{\alpha-1} \hat{B}^{\beta} \tag{16}$$

where α, β and C_{s} stand for the material-dependent Steinmetz parameters identified for purely sinusoidal changes of the magnetization state. This also constitutes the primary advantage of this modeling approach, as only well-known and standardized measurements with purely sinusoidal flux densities are necessary for a complete identification. Another example for a modified iron loss model is the Generalized Steinmetz Equation (GSE). According to [39], the authors enhance the main idea of MSE and define the instantaneous iron losses as a single-valued function that is only dependent on the material itself, the magnetic flux density $B(t)$ as well as on its rated change $\frac{\mathrm{d}B(t)}{\mathrm{d}t}$. Based on this hypothesis, a formula can be derived that allows estimating the iron losses by evaluating

$$p_{\mathrm{fe}} = \frac{1}{T} \int_0^T C_{\mathrm{s,m}} \left|\frac{\mathrm{d}B(t)}{\mathrm{d}t}\right|^{\alpha} |B(t)|^{\beta-\alpha} \mathrm{d}t \tag{17}$$

In (17), the modeling parameter $C_{\mathrm{s,m}}$ is a modified Steinmetz coefficient that can be calculated by reusing the coefficients for sinusoidal flux density characteristics. Therefore, it was one of the first approaches, which uses temporal magnetic field courses for the estimation of instantaneous iron loss in the material. Especially for ferrimagnetic materials, such as ferrites, additional modifications of the Steinmetz equation are developed. For instance, the Improved Generalized Steinmetz equations (iGSE, [60]) or the Natural Steinmetz equation (NSE, [59]) were presented in the past.

2.3 Hysteresis models for alternating magnetization

All models described so far either estimate the nonlinear relationship of the magnetic field quantities B and H or the iron losses caused by the coupling of these magnetic fields inside the material. As aforementioned and depicted by (4) and (6), the specific instantaneous power loss and the relationship of magnetic flux density and magnetic field strength, described by the B-H curve, are not separate phenomena. Both are due to the interaction of the dynamic magnetization process of the material and the external magnetic fields, which becomes visible in form of the nonlinear hysteresis curve. Thus, many researchers focus on directly modeling the magnetic hysteresis loop to obtain an appropriate material characterization. The most frequently applied hysteresis model in finite element (FE) simulations for many electromagnetic problems are the discrete Preisach model [46] and the hysteresis model according to Jiles and Atherton [34]. Both models determine the magnetization M instead of B, and the B-H curve can be calculated by taking advantage of the relationship $B = \mu_0(H + M(H))$, where μ_0 is the vaccum permeability. The discrete Preisach hysteresis model is based on the classic Preisach model introduced in [46]. It subdivides ferromagnetic materials in N magnetic domains, so called hysterons, with different properties. Each hysteron represents a memory of the current magnetization state of the given domain. Usually, the magnetic behavior of each hysteron $i = 1..N$ is described by a simple rectangular hysteresis loop with individually defined thresholds a_{i} and b_{i} as well as a particular scaling factor m_{i}. In case of the discrete Preisach model, the contributions of the outputs of all hysterons are summed up to form the total magnetization of the material. Figure 3 shows the basic concept of the discrete Preisach hysteresis model. In order to achieve high modeling accuracy, a large number of domains and hence many modeling parameters are used. Consequently, for a complete identification of the hysteresis model, many independent measurements are required.

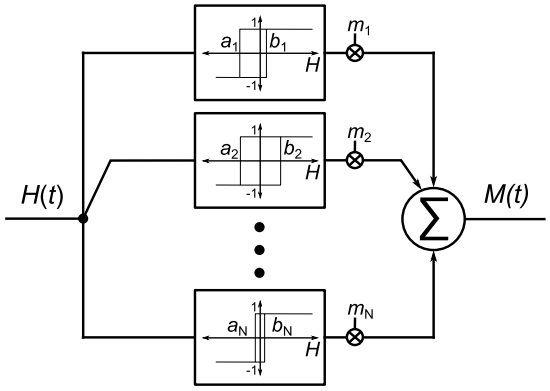

Figure 3: Basic concept of the discrete Preisach hysteresis model consisting of N hysterons.

Additionally, some extensions and modifications of the classic Preisach model have been developed, such as the dynamic Preisach model, the magnetodynamic viscosity based model and, the loss surface model. Krings et al. discuss their basic principles and compare them in [36]. In contrast to the Preisach model, the fundamental idea of the Jiles-Atherton hysteresis model [34] is the subdivision of the magnetization $M = M_{\mathrm{rev}} + M_{\mathrm{irr}}$, where M_{rev} is a reversible component and M_{irr} an irreversible component. Due to assumptions made in [34] and [7], both are linked with the effective magnetization force $H_{\mathrm{e}} = H + \alpha M$ inside the material by

$$M_{\mathrm{rev}} = c(M_{\mathrm{an}} - M_{\mathrm{irr}}) \tag{18}$$

and

$$\frac{\mathrm{d}M_{\mathrm{irr}}}{\mathrm{d}H_{\mathrm{e}}} = \frac{M_{\mathrm{an}} - M_{\mathrm{irr}}}{k\delta}, \tag{19}$$

where the parameter $\delta = \pm 1$ defines whether the given loop branch ascends or descends. The anhysteretic magnetization M_{an} of the material is modeled by a modified Langevin approach, similar to (1), and thus can be written as

$$M_{\mathrm{an}} = M_{\mathrm{s}} \left(\coth\left(\frac{H_{\mathrm{e}}}{a}\right) - \frac{a}{H_{\mathrm{e}}} \right). \tag{20}$$

The additional parameters c, k, M_{s}, a, and α in (18)–(20) define the given material properties and are identified by measurements. According to (19), an ordinary first-order differential equation is solved to predict all terms of the resulting magnetization $M = M_{\mathrm{irr}} + c(M_{\mathrm{an}} - M_{\mathrm{irr}})$ as a nonlinear and hysteretic function of H in each node of a mesh. A detailed comparison of the Jiles-Atherton model with the Preisach model can be found in [7]. On the one hand, the Jiles-Atherton hysteresis model bears more relation to the underlying physical principles, it needs significantly fewer modeling parameters, it is easier to identify, and it typically takes less computing time considering numerical field computations. On the other hand, results calculated with the Preisach model are usually more accurate [7]. Nevertheless, both models require a significant amount of measuring data compared to the models discussed in Section 2.2 and their identification and implementation for numeric simulation is more time-consuming.

2.4 General and novel approach for alternating iron loss and magnetization curve modeling

If the magnetic behavior of a material is described using a hysteresis-curve model, the energy loss per volume can be calculated by integrating B along the identified hysteresis curve as described in (3). Consequently, the signals $B(t)$ and $H(t)$ in each volume element, as well as at any time are necessary to determine the individual magnetization state and its temporal change. Many electromagnetic devices are evaluated using magnetostatic tools. Hence, the temporal courses of the field quantities are usually unknown. In addition, a modeling error in the hysteresis model at one particular time instant can permanently impact the accuracy of the magnetization state determination at any subsequent point in time. As a result, both the predicted operating point of the material and the consequently derived instantaneous iron losses can feature unfeasibly large errors. For this reason, the authors in [11] suggest jointly modeling losses and material characteristics using a quasi time-invariant model

$$p_{\mathrm{fe}}(t) = p\left(B(t), \tfrac{\mathrm{d}B(t)}{\mathrm{d}t}\right), \tag{21}$$

where p is a two-dimensional function depending on the current state of $B(t)$ and its rated change $\frac{\mathrm{d}B(t)}{\mathrm{d}t}$. On the one hand, the instantaneous power loss for given $B(t)$ and $\frac{\mathrm{d}B(t)}{\mathrm{d}t}$ can be determined by using (21). On the other hand, $H(t)$ can also be estimated by merging the formula for instantaneous power loss (21) and (6) to

$$H(t) = p\left(B(t), \tfrac{\mathrm{d}B(t)}{\mathrm{d}t}\right)\left(\tfrac{\mathrm{d}B(t)}{\mathrm{d}t}\right)^{-1}. \tag{22}$$

Hence, the entire information about the magnetization state of the material as well as the instantaneous iron losses can be derived by applying a single material-specific 2D-function that is determined using measurement data. Additionally, the authors suggest triangle-shaped flux densities for the measurements. Thus, the material exhibits different magnetic flux densities at a constant $\frac{\mathrm{d}B(t)}{\mathrm{d}t}$ level. If the frequency of the waveform is varied, a spe-

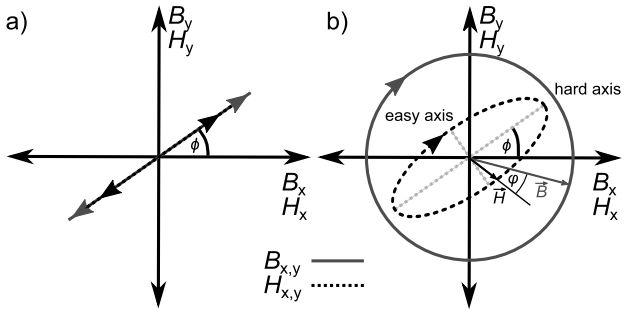

Figure 4: Comparison of the resulting flux densities under alternating and rotational magnetization: **a)** Alternating flux condition in the direction of maximal magnetic flux density marked by the inclination angle Φ. **b)** Rotational flux condition under rotational magnetization with a hard axis direction indicated by inclination angle Φ.

cific $(B(t), \frac{\mathrm{d}B(t)}{\mathrm{d}t})$-grid can be analyzed and thus the domain used for modeling is explored best. The model was verified by triangular B characteristics and B waveforms comprising a fundamental wave and a third harmonic. Overall, the maximum detected modeling error did not exceed 5 %. In contrast to the Preisach- or Jiles-Atherton hysteresis model, a modeling error at a particular time instant does not directly affect any other subsequent moment in time.

2.5 Vector magnetic modeling of magnetic properties and iron losses for rotational and multi-dimensional magnetization

In addition to the alternating (i. e., one-dimensional) magnetization, a rotational and multi-dimensional magnetization occurs in certain regions of electromagnetic devices, as described in Section 2.2.1. Due to the microstructure given by the manufacturing process, many electrical sheets exhibit a magnetic anisotropy. As a result, the two-dimensional magnetic characteristics of the sheet has a magnetically preferred spatial direction, called easy axis. In contrast, the hard axis represents the direction that is most difficult to magnetize. Because of the anisotropy, the magnitude of the resulting magnetic field depends on the local magnetization direction. Figure 4 compares the loci of the vectors of $\vec{B}$ and $\vec{H}$ for both 1D- and 2D-magnetization. Beside the spatial dependency of the magnitude, two-dimensional measurements show a phase difference ϕ between $\vec{B}$ and $\vec{H}$ vector, as a result of the anisotropy. If no alternating magnetization can be assumed in the material, the magnetic anisotropy, the magnetic nonlinearity, and the phase lag must be considered in the modeling approach in order to precisely estimate the local iron losses. For example, Enokizono et al. introduced and discussed a vector-based magnetic model for two-dimensional magnetization in [22] and [52]. The prediction of the anisotropic nonlinear magnetic characteristics as well as the spatial distribution of the iron losses agree well with measurements. Furthermore, the above-mentioned hysteresis models have been extended to vectorial formulations in order to represent magnetic anisotropy in complex hysteresis models as well [42, 8]. Further approaches and explanations, can be found for instance in [41, 43, 66].

3 Characterization of the manufacturing impact on the B-H curve

Thanks to increases in computational power, the modeling and optimization of electrical machines saw a significant boost throughout the last decades. Evermore complex nonlinear modeling strategies are applied. In addition, high throughput computing software, e. g., HTCondor [58], allows investigating thousands of designs within reasonable time. As the minimization of the cost of the device is typically a top priority objective [12], highly utilized designs are obtained when applying the aforementioned measures. To avoid unwanted surprises when performing measurements for built prototypes, the accuracy of material characterization continuously requires improvement. A significant aspect is to investigate the impact of manufacturing on local properties of soft magnetic materials. The considered techniques can be subdivided into two categories. The first one is about the realization of the shaping of the cross section of the considered machine design or device, while the other is the stacking and fixing of the lamination sheets. Moreover, the pressing of the stacked arrangement into supportive machine components, e. g., aluminum housing, takes effect on the material characteristics. Typical shaping processes are punching, laser cutting, and wire eroding. The first one is usually considered for mass-produced components. Stacking can be realized by applying interlocks, welding, or gluing. While the lamination sheets can be glued during manufacturing, a more efficient way is to consider self-bonding laminations. Thereby, a thin layer of glue is applied on a single side of the lamination sheet during the manufacturing of the soft magnetic material. Employed processes depend very strongly on the desired performance and cost of the given magnetic circuit.

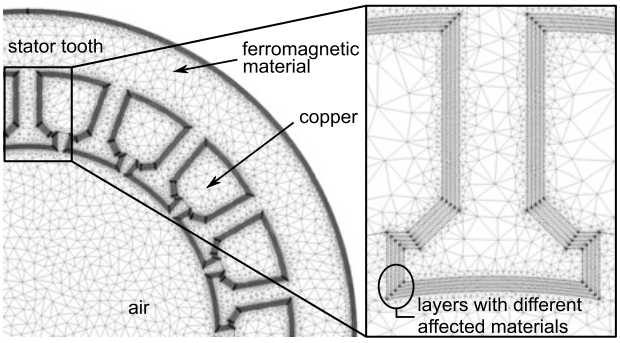

Figure 5: A layer-based approach with $n = 5$ layers for modeling the impact of manufacturing on the material characteristics close to the respective material cutting edge.

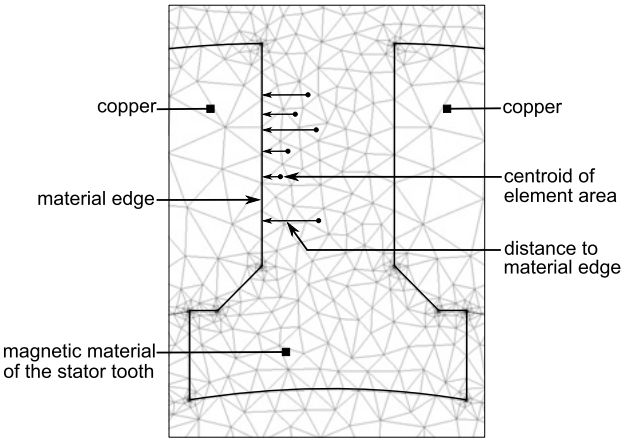

Figure 6: A continuous modeling approach of manufacturing impact on material properties close to the cutting edge.

3.1 Shaping of the machine design cross section and its impact on material characteristics

The shaping of the cross section usually affects the material properties along the cut edges. Depending on the chemical composition and process treatment of the material, the layer thickness, and the applied shaping technique, significant decrease of the material properties is observed up to a distance of 2–3 mm from the cut edge [40, 6, 61]. In case of punching, the change is mainly due to residual mechanical stress and plastic deformation of the material [38, 26, 15, 63, 56], while for laser cutting it is due to thermal effects [21, 3]. Stress relief annealing can be applied to at least partly restore the material characteristics [10, 16]. By contrast, electrical discharge machining (EDM), also known as wire cutting, shows significantly lower impact on the material [17]. A comparison of different shaping techniques can be found in [4]. Especially for small-size magnetic apparatuses, e. g., fractional horsepower machines with overall small dimensions, the change of the material characteristics has significant impact on the overall performance of the machine. Thus, researchers carried out investigations to measure the manufacturing effects and, consequently, to find models suitable for machine design analysis, preferably for both analytical models as well as for finite element analysis software [5, 48]. Among the plethora of presented techniques, two main directions of research can be observed. A layer-based approach [2] or an element-wise assignment of material properties considering their distance to the cut edge [20, 28, 50]. The first one can be applied for both, analytic models as well as FE tools. An example of the stator teeth section and n layers is presented in Fig. 5. Development of techniques for an element-wise assignment is particularly devoted for finite element software application. Thereby, the material cross section is inherently discretized into the finite elements. Sophisticated and typically customized modeling environments allow for such an element-wise assignment of material parameters [53, 54, 55]. Figure 6 gives an example for this approach. Typically, the centroid of the triangle is used for defining its distance to the cut edge. Both, an individual material definition per element or a discretization of the affected zone to n layers and, consequently, n different materials, is reasonable. A big advantage of the element-wise assignment compared to introducing layers is that the zone close to the cut edge does not necessarily need to be discretized to very small finite elements. Based on requirements regarding computational cost and modeling accuracy, a reasonable discretization can be defined. As the consideration of the manufacturing impact currently is a major topic, selected references only constitute a small excerpt of the recently published studies. Needless to say that, research in this field is still ongoing.

3.2 Change of material properties due to stacking and fixing of lamination sheets

While for the field covered by Section 3.1 multitudinous activities can be experienced, the topic of this section is not so extensively investigated. Thus, a rather limited number of general models covering the effects due to fixing the steel sheets during the stacking process is available. Some examples about welding and clamping can be found in [25]. Moreover, the pressing of a stator into an aluminum housing is investigated in [27].

4 Conclusions and outlook

Because of advances in numerical techniques for evaluating electromagnetic devices and increase in computational power, optimization of these components currently is a major topic in electrical engineering. If the tools are applied, highly-utilized designs are obtained, where materials are driven up to very high flux density amplitudes and thus highly nonlinear characteristics are observed. This increases requirements on modeling the material properties and thus extensive research activities continue to be carried out. This article gives a comprehensive overview of main research directions for modeling both the hysteretic behavior as well as the loss due to magnetization state changes of ferromagnetic materials. The focus is on techniques that can be applied in common tools used for electromagnetic device characterization, e. g., the finite element method. Besides obtaining the performance of materials for rated conditions, the impact of manufacturing is a further crucial topic allowing to obtain accurate results when investigating the characteristics of electromagnetic devices. Especially throughout the last couple of years, significant advances in modeling the effect of manufacturing techniques for shaping and stacking the steel laminations have been achieved. This manuscript gives a one-stop reference for readers to get a wide overview of overall available models for characterizing the electromagnetic performance of ferromagnetic materials. Most prominent and typically applied techniques are focused. Besides, a comprehensive list of state-of-the-art references is mentioned that allows for delving into this exciting and ongoing topic of research.

Funding: This work has been supported by the COMET-K2 "Center for Symbiotic Mechatronics" of the Linz Center of Mechatronics (LCM) funded by the Austrian federal government and the federal state of Upper Austria.

References

1. D. Andessner, R. Kobler, J. Passenbrunner, and W. Amrhein. Measurement of the magnetic characteristics of soft magnetic materials with the use of an iterative learning control algorithm. *2011 IEEE Vehicle Power and Propulsion Conference, VPPC 2011*, pages 1–6, 2011.
2. M. Bali, H. De Gersem, and A. Muetze. Finite-element modeling of magnetic material degradation due to punching. *IEEE Transactions on Magnetics*, 50(2):745–748, 2014.
3. M. Bali, H. De Gersem, and A. Muetze. Determination of Original Nondegraded and Fully Degraded Magnetic Characteristics of Material Subjected to Laser Cutting. *IEEE Transactions on Industry Applications*, 53(5):4242–4251, 2017.
4. M. Bali and A. Muetze. Influences of CO2 Laser, FKL Laser, and Mechanical Cutting on the Magnetic Properties of Electrical Steel Sheets. *IEEE Transactions on Industry Applications*, 51(6):4446–4454, 2015.
5. M. Bali and A. Muetze. Modeling the Effect of Cutting on the Magnetic Properties of Electrical Steel Sheets. *IEEE Transactions on Industrial Electronics*, 64(3):2547–2556, 2017.
6. M. Bali and A. Muetze. The degradation depth of non-grain oriented electrical steel sheets of electric machines due to mechanical and laser cutting: A state-of-the-art review. *IEEE Transactions on Industry Applications*, 55(1):366–375, 2019.
7. A. Benabou, S. Clénet, and F. Piriou. Comparison of Preisach and Jiles-Atherton models to take into account hysteresis phenomenon for finite element analysis. *Journal of Magnetism and Magnetic Materials*, 2003.
8. A.J. Bergqvist. A simple vector generalization of the Jiles-Atherton model of hysteresis. *IEEE Transactions on Magnetics*, 32(5):4213–4215, 1996.
9. G. Bertotti. Physical interpretation of eddy current losses in ferromagnetic materials. I. Theoretical considerations. *Journal of Applied Physics*, 57(6):2110–2117, mar 1985.
10. R. Bojoi, A. Cavagnino, Z. Gmyrek, and M. Lefik. Post-annealing behaviors of small-size synchronous reluctance motors. In *IECON 2016 – 42nd Annual Conference of the IEEE Industrial Electronics Society*, pages 1732–1737. IEEE, oct 2016.
11. G. Bramerdorfer and D. Andessner. Accurate and Easy-to-Obtain Iron Loss Model for Electric Machine Design. *IEEE Transactions on Industrial Electronics*, 64(3):2530–2537, 2017.
12. G. Bramerdorfer, S. Silber, G. Weidenholzer, and W. Amrhein. Comprehensive cost optimization study of high-efficiency brushless synchronous machines. *Proceedings of the 2013 IEEE International Electric Machines and Drives Conference, IEMDC 2013*, 2017(January):1126–1131, 2013.
13. J.R. Brauer. Simple Equations for the Magnetization and Reluctivity Curves of Steel. *IEEE Transactions on Magnetics*, 11(1):81, 1975.
14. L. Chang, T.M. Jahns, and R. Blissenbach. Characterization and modeling of soft magnetic materials for improved estimation of pwm-induced iron loss. In *2018 IEEE Energy Conversion Congress and Exposition (ECCE)*, pages 5371–5378, 09 2018.
15. C.C. Chiang, M.F. Hsieh, Y.H. Li, and M.C. Tsai. Impact of Electrical Steel Punching Process on the Performance of Switched Reluctance Motors. *IEEE Transactions on Magnetics*, 51(11):1–4, 2015.
16. M. Cossale, G. Bramerdorfer, G. Goldbeck, M. Kitzberger, D. Andessner, and W. Amrhein. Modeling the Degradation of Relative Permeability in Soft Magnetic Materials. In *2018 IEEE Transportation and Electrification Conference and Expo, ITEC 2018*, pages 744–748, 2018.
17. M. Cossale, M. Kitzberger, G. Goldbeck, G. Bramerdorfer, D. Andessner, and W. Amrhein. Investigation and Modeling of Local Degradation in Soft Magnetic Materials. In *2018 IEEE Energy Conversion Congress and Exposition (ECCE)*, pages 5365–5370. IEEE, sep 2018.
18. P. Diez. Symmetric invertible *b–h* curves using piecewise linear rationals. *IEEE Transactions on Magnetics*, 53(6):1–3, June 2017.

19. P. Diez and J.P. Webb. A rational approach to *b–h* curve representation. *IEEE Transactions on Magnetics*, 52(3):1–4, March 2016.
20. S. Elfgen, S. Steentjes, S. Böhmer, D. Franck, and K. Hameyer. Continuous Local Material Model for Cut Edge Effects in Soft Magnetic Materials. *IEEE Transactions on Magnetics*, 2016.
21. S. Elfgen, S. Steentjes, S. Bohmer, D. Franck, and K. Hameyer. Influences of Material Degradation Due to Laser Cutting on the Operating Behavior of PMSM Using a Continuous Local Material Model. *IEEE Transactions on Industry Applications*, 53(3):1978–1984, may 2017.
22. M. Enokizono. Vector magnetic property and magnetic characteristic analysis by vector magneto-hysteretic E and S model. *IEEE Transactions on Magnetics*, 2009.
23. J. Epstein. Die magnetische prufung von eisenblech. *Elektrotechnische Zeitschrift*, pages 303–307, 1900.
24. B. Forghani, E.M. Freeman, D.A. Lowther, and P.P. Silvester. Interactive Modelling of Magnetisation Curves. *IEEE Transactions on Magnetics*, 18(6):1070–1072, 1982.
25. Z. Gmyrek and A. Cavagnino. Influence of punching, welding, and clamping on magnetic cores of fractional kilowatt motors. *IEEE Transactions on Industry Applications*, 54(5):4123–4132, Sep. 2018.
26. Z. Gmyrek, A. Cavagnino, and L. Ferraris. Estimation of the Magnetic Properties of the Damaged Area Resulting From the Punching Process: Experimental Research and FEM Modeling. *IEEE Transactions on Industry Applications*, 49(5):2069–2077, sep 2013.
27. P. Goes, E. Hoferlin, and M. De Wulf. Calculating Iron Losses Taking Into Account Effects of Manufacturing Processes. *Journal of The Electrochemical Society*, 104(12):256C, 1957.
28. G. Goldbeck, M. Cossale, M. Kitzberger, G. Bramerdorfer, D. Andessner, and W. Amrhein. Numerical Implementation of Local Degradation Profiles in Soft Magnetic Materials. In *Proceedings – 2018 23rd International Conference on Electrical Machines, ICEM 2018*, pages 1037–1043, 2018.
29. T. Hülsmann. *Nonlinear Material Curve Modeling and Sensitivity Analysis for MQS-Problems*. PhD thesis, Bergische Universität Wuppertal, 2012.
30. International Electrotechnical Commission. Magnetic materials – part 2: Methods of measurement of the magnetic properties of electrical steel strip and sheet by means of an epstein frame, June 2008.
31. International Electrotechnical Commission. Magnetic materials – part 4: Methods of measurement of the magnetic properties of magnetic sheet and strip by means of a single sheet tester, April 2010.
32. International Electrotechnical Commission. Magnetic materials – part 6: Methods of measurement of the magnetic properties of magnetically soft metallic and powder materials at frequencies in the range 20 Hz to 100 kHz by the use of ring specimens, May 2018.
33. S. Jacobs, D. Hectors, F. Henrotte, M. Hafner, M.H. Gracia, K. Hameyer, and P. Goes. Magnetic material optimization for hybrid vehicle PMSM drives. *World Electric Vehicle Journal*, 2009.
34. D.C. Jiles and D.L. Atherton. Theory of ferromagnetic hysteresis. *Journal of Magnetism and Magnetic Materials*, 1986.
35. P. Jordan. Die ferromagnetischen Konstanten für schwache Wechselfelder. *Elektr. Nach. Techn.*, 1:8, 1924.
36. A. Krings and J. Soulard. Overview and Comparison of Iron Loss Models for Electrical Machines. *Journal of Electrical Engineering*, 2010.
37. J.C. Lagarias, J.A. Reeds, M.H. Wright, and P.E. Wright. Convergence Properties of the Nelder-Mead Simplex Method in Low Dimensions. *SIAM Journal of Optimization*, 9(1):112–147, 1998.
38. N. Leuning, S. Steentjes, H.A. Weiss, W. Volk, and K. Hameyer. Magnetic Material Deterioration of Non-Oriented Electrical Steels as a Result of Plastic Deformation Considering Residual Stress Distribution. *IEEE Transactions on Magnetics*, 54(11):1–5, nov 2018.
39. J. Li, T. Abdallah, and C.R. Sullivan. Improved calculation of core loss with nonsinusoidal waveforms. In *Conference Record of the 2001 IEEE Industry Applications Conference. 36th IAS Annual Meeting*, volume 4, pages 2203–2210. IEEE, 2001.
40. G. Loisos and A.J. Moses. Effect of mechanical and Nd:YAG laser cutting on magnetic flux distribution near the cut edge of non-oriented steels. *Journal of Materials Processing Technology*, 2005.
41. I.D. Mayergoyz. Vector Preisach hysteresis models (invited). *Journal of Applied Physics*, 1988.
42. I.D. Mayergoyz. *Mathematical Models of Hysteresis and Their Applications*. Elsevier, 2003.
43. W.H.F. Murdoch. Magnetic Measurements. *Nature*, 96(2395):87–87, sep 1915.
44. H. Pfützner. Zur Bestimmung der Ummagnetisierungsverluste aus den Feldgrößen. *Archiv für Elektrotechnik*, 60(3):177–179, may 1978.
45. N.C. Pop and O.F. Caltun. Jiles-Atherton magnetic hysteresis parameters identification. *Acta Physica Polonica A*, 120(3):491–496, 2011.
46. F. Preisach. Über die magnetische Nachwirkung. *Zeitschrift für Physik*, 1935.
47. B. Sai Ram and S.V. Kulkarni. An isoparametric approach to model ferromagnetic hysteresis including anisotropy and symmetric minor loops. *Journal of Magnetism and Magnetic Materials*, 474:574–584, 2019.
48. P. Rasilo, S. Steentjes, A. Belahcen, R. Kouhia, and K. Hameyer. Model for Stress-Dependent Hysteresis in Electrical Steel Sheets Including Orthotropic Anisotropy. *IEEE Transactions on Magnetics*, 53(6):1–4, 2017.
49. J. Reinert, A. Brockmeyer, and R.W.A.A. De Doncker. Calculation of losses in ferro- and ferrimagnetic materials based on the modified Steinmetz equation. *IEEE Transactions on Industry Applications*, 37(4):1055–1061, 2001.
50. B. Schauerte, S. Steentjes, N. Leuning, and K. Hameyer. A continuous parameter-based approach to model the effect of mechanical stress on the electromagnetic hysteresis characteristic. In *2018 IEEE International Magnetics Conference (INTERMAG)*, pages 1–5, April 2018.
51. R. Severns. HF-core losses for nonsinusoidal waveforms. In *High Frequency Power Convertion Conference (HFPC)*, pages 140–148, 1991.
52. H. Shimoji, M. Enokizono, T. Todaka, and T. Honda. A new modeling of the vector magnetic property. *IEEE Transactions on Magnetics*, 38(2):861–864, mar 2002.
53. S. Silber, G. Bramerdorfer, A. Dorninger, A. Fohler, J. Gerstmayr, W. Koppelstätter, D. Reischl, G. Weidenholzer, and S. Weitzhofer. Coupled optimization in MagOpt. *Proceedings*

of the Institution of Mechanical Engineers. Part I: Journal of Systems and Control Engineering, 230(4):291–299, 2015.

54. S. Silber, W. Koppelstätter, G. Weidenholzer, and G. Bramerdorfer. MagOpt – Optimization tool for mechatronic components. *14th International Symposium on Magnetic Bearings*, 4:243–246, 2014.
55. S. Silber, W. Koppelstätter, G. Weidenholzer, G. Segon, and G. Bramerdorfer. Reducing Development Time of Electric Machines with SyMSpace. In *2018 8th International Electric Drives Production Conference (EDPC)*, pages 1–5. IEEE, dec 2018.
56. S. Steentjes, N. Leuning, J. Dierdorf, X. Wei, G. Hirt, H.A. Weiss, W. Volk, S. Roggenbuck, S. Korte-Kerzel, A. Stoecker, R. Kawalla, and K. Hameyer. Effect of the Interdependence of Cold Rolling Strategies and Subsequent Punching on Magnetic Properties of NO Steel Sheets. *IEEE Transactions on Magnetics*, 52(5):1–4, may 2016.
57. C.P. Steinmetz. On the law of hysteresis. *Proceedings of the IEEE*, 72(2):197–221, 1984.
58. T. Tannenbaum, D. Wright, K. Miller, and M. Livny. Condor – a distributed job scheduler. In Thomas Sterling, editor, *Beowulf Cluster Computing with Linux*. MIT Press, October 2001.
59. A. Van den Bossche, V.C. Valchev, and G.B. Georgiev. Measurement and loss model of ferrites with non-sinusoidal waveforms. In *2004 IEEE 35th Annual Power Electronics Specialists Conference*, number 1, pages 4814–4818. IEEE, 2004.
60. K. Venkatachalam, C.R. Sullivan, T. Abdallah, and H. Tacca. Accurate prediction of ferrite core loss with nonsinusoidal waveforms using only Steinmetz parameters. In *2002 IEEE Workshop on Computers in Power Electronics, 2002. Proceedings*, pages 36–41. IEEE, 2002.
61. H.A. Weiss, P. Trober, R. Golle, S. Steentjes, N. Leuning, S. Elfgen, K. Hameyer, and W. Volk. Impact of Punching Parameter Variations on Magnetic Properties of Nongrain-Oriented Electrical Steel. *IEEE Transactions on Industry Applications*, 54(6):5869–5878, nov 2018.
62. P.R. Wilson, J.N. Ross, A.D. Brown, T. Kazmierski, and J. Baranowski. Efficient Mixed-Domain Behavioural Modeling of Ferromagnetic Hysteresis Implemented in VHDL-AMS 3. Implementing the Original Jiles-Atherton. *Optimization*, 44(0):4–5, 2004.
63. R. Woehrnschimmel, A. Muetze, S. Ertl, H. Kapeller, O. Winter, and D. Horwatitsch. Simulating the change of magnetic properties of electrical steel sheets due to punching. In *2015 IEEE International Electric Machines & Drives Conference (IEMDC)*, pages 1324–1328. IEEE, may 2015.
64. T. Yamamoto and Y. Ohya. Single Sheet Tester for Measuring Core Losses and Permeabilities in a Silicon Steel Sheet. *IEEE Transactions on Magnetics*, 10(2):157–159, 1974.
65. S.E. Zirka, Y.I. Moroz, S. Steentjes, K. Hameyer, K. Chwastek, S. Zurek, and R.G. Harrison. Dynamic magnetization models for soft ferromagnetic materials with coarse and fine domain structures. *Journal of Magnetism and Magnetic Materials*, 394:229–236, 2015.
66. S. Zurek. *Characterisation of Soft Magnetic Materials Under Rotational Magnetisation*. CRC Press, Boca Raton: Taylor & Francis, CRC Press, nov 2017.

Bionotes

Gerd Bramerdorfer
Johannes Kepler University Linz, Department of Electrical Drives and Power Electronics, Altenbergerstraße 69, 4040 Linz, Austria
gerd.bramerdorfer@jku.at

Gerd Bramerdorfer received the Ph. D. degree in electrical engineering from Johannes Kepler University Linz, Linz, Austria, in 2014. He is currently an Assistant Professor with the Department of Electrical Drives and Power Electronics, Johannes Kepler University Linz. His current research interests include the design, modeling, and optimization of electric machines as well as magnetic bearings and bearingless machines. Dr. Bramerdorfer is a Senior Member of the IEEE (2018), the IEEE Industrial Electronics Society, the IEEE Industry Applications Society, and the IEEE Magnetics Society. He serves for the scientific community as a Guest Editor, a Track Chair, a Topic Chair, and by organizing special sessions. He is a reviewer for international journals and conferences. He is an Associate Editor of the IEEE Transactions on Industrial Electronics.

Martin Kitzberger
Johannes Kepler University Linz, Department of Electrical Drives and Power Electronics, Altenbergerstraße 69, 4040 Linz, Austria
martin.kitzberger@live.com

Martin Kitzberger was born in Linz, Austria, in 1990. He received the Dipl.-Ing degree in Mechatronics in 2016 and is engaged as a scientific researcher at the Institute for Electrical Drives and Power Electronics of Johannes Kepler University Linz since then. His field of research includes electrical drives and power electronics, magnetic material characterization and material modeling.

Daniel Wöckinger
Johannes Kepler University Linz, Department of Electrical Drives and Power Electronics, Altenbergerstraße 69, 4040 Linz, Austria
daniel.woeckinger@jku.at

Daniel Wöckinger was born in Linz, Austria in 1991. He received his master degree in mechatronics at the University of Linz, Austria in 2017. He is currently working toward the Ph. D. degree at JKU. Since 2017 he has been with the Institute of Electrical Drives and Power Electronics, Johannes Kepler University Linz. His research interests include magnetic measuring systems, eddy current testing and modeling of electromagnetic materials.

Branko Koprivica
University of Kragujevac, Faculty of Technical Sciences in Cacak, Svetog Save 65, 32000 Cacak, Serbia
branko.koprivica@ftn.kg.ac.rs

Branko Koprivica received the Ph. D. degree in electrical engineering from University of Kragujevac, Serbia, in 2015. He is currently an Assistant Professor with the Department of Electrical and Electronic Engineering, Faculty of Technical Sciences in Cacak, University of Kragujevac, Serbia. His current research interests include numerical methods in electromagnetics, magnetism and magnetic measurements, metrology of electrical and non-electrical quantities, sensors and remote experiments.

Stan Zurek
Megger Instruments Ltd, Archcliffe Road, CT17 9EN Dover, UK
stan.zurek@ieee.org

Stan Zurek graduated at Czestochowa University of Technology, and completed his PhD degree at Wolfson Centre for Magnetics, Cardiff University, UK in 2005, where he continued to work as a Research Associate. In 2008 he joined Megger Instruments Ltd where he currently holds the position of Head of Research & Innovation, being responsible for all aspects of electromagnetics and new technologies. He was elevated to IEEE Senior Member in 2010. He is an author and co-author of over 60 publications, and holds 5 patents. Recently he published a comprehensive book on measurements of rotational power loss: “Characterisation of Soft Magnetic Materials Under Rotational Magnetisation”.